Supplementary information

Impact of lanthanum ion exchange and steaming dealumination on middle distillate production using nanosized Y zeolite catalyst in hydrocracking reaction

Carlos Mendoza [a*] Cecilia Manrique[a*], Adriana Echavarría[a*]

[a] Grupo Catalizadores y Adsorbentes, Instituto de Química, Universidad de Antioquia, Calle 70 No. 52-21, Medellín, Colombia

Corresponding author. Tel.: +57 604 219 5653; postal address 050010, Calle 67 No 53-108, Medellín, Colombia

*E-mail address: cjavier.mendoza@udea.edu.co, alba.manrique@udea.edu.co, adriana.echavarria@udea.edu.co

a)

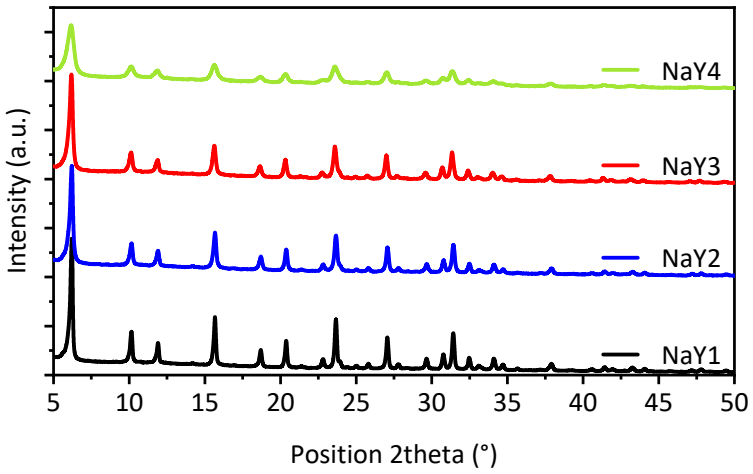

b)

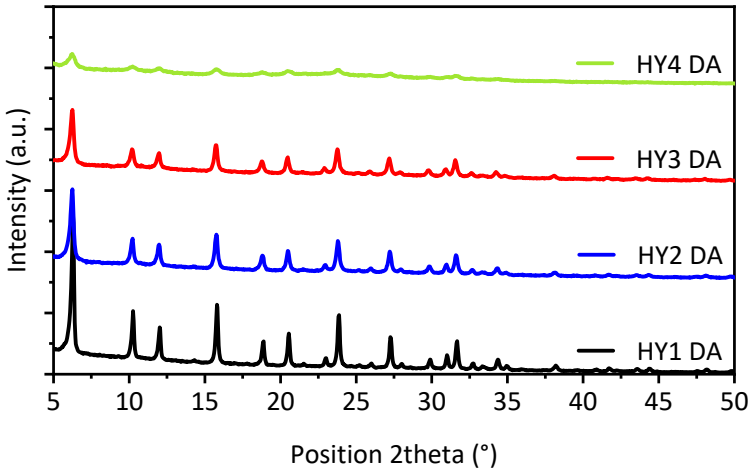

c)

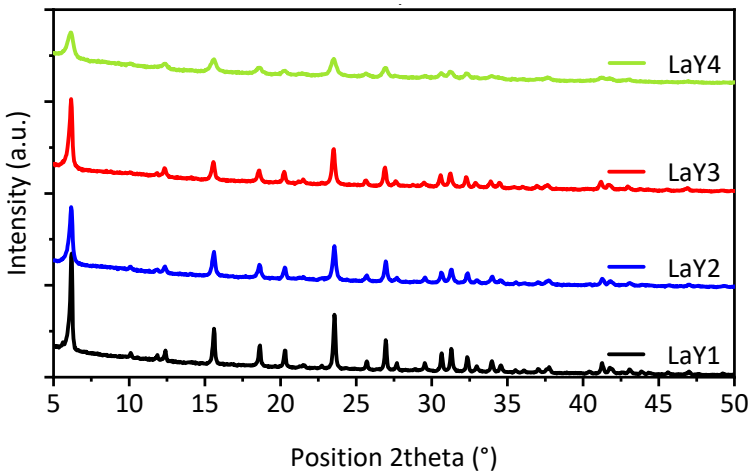

Figure S1. XRD patter of synthesized zeolites a) NaY, b) HYDA and c) LaY

NaY1

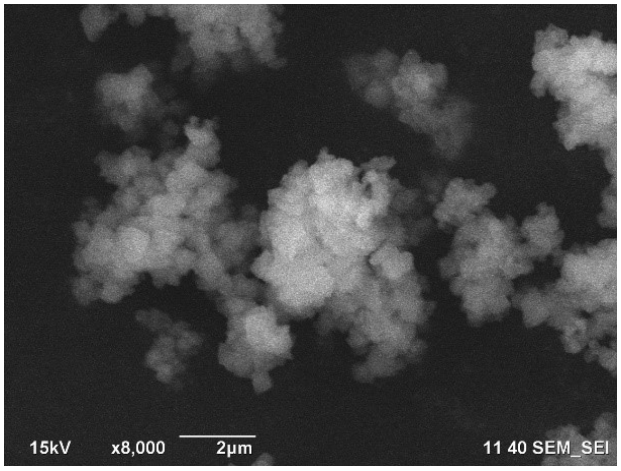

NaY2

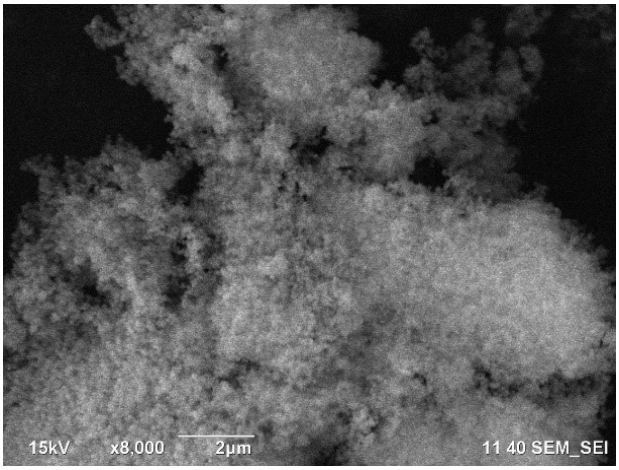

NaY3

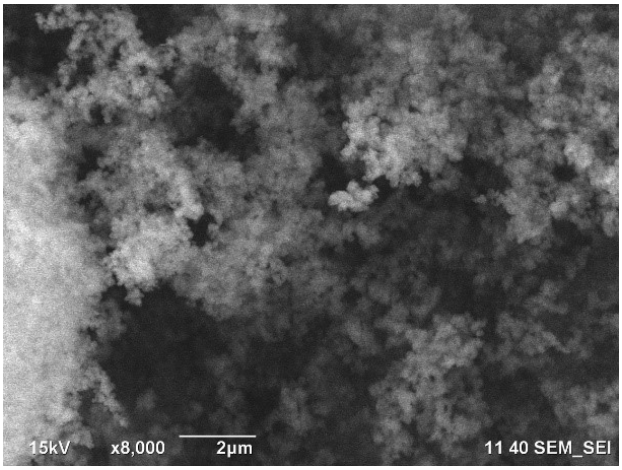

NaY4

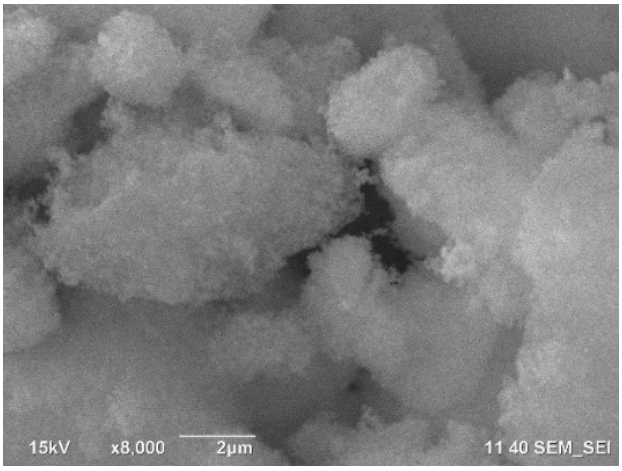

Figure S2. SEM images of synthesized zeolites NaY1, NY2, NaY3 and NaY4

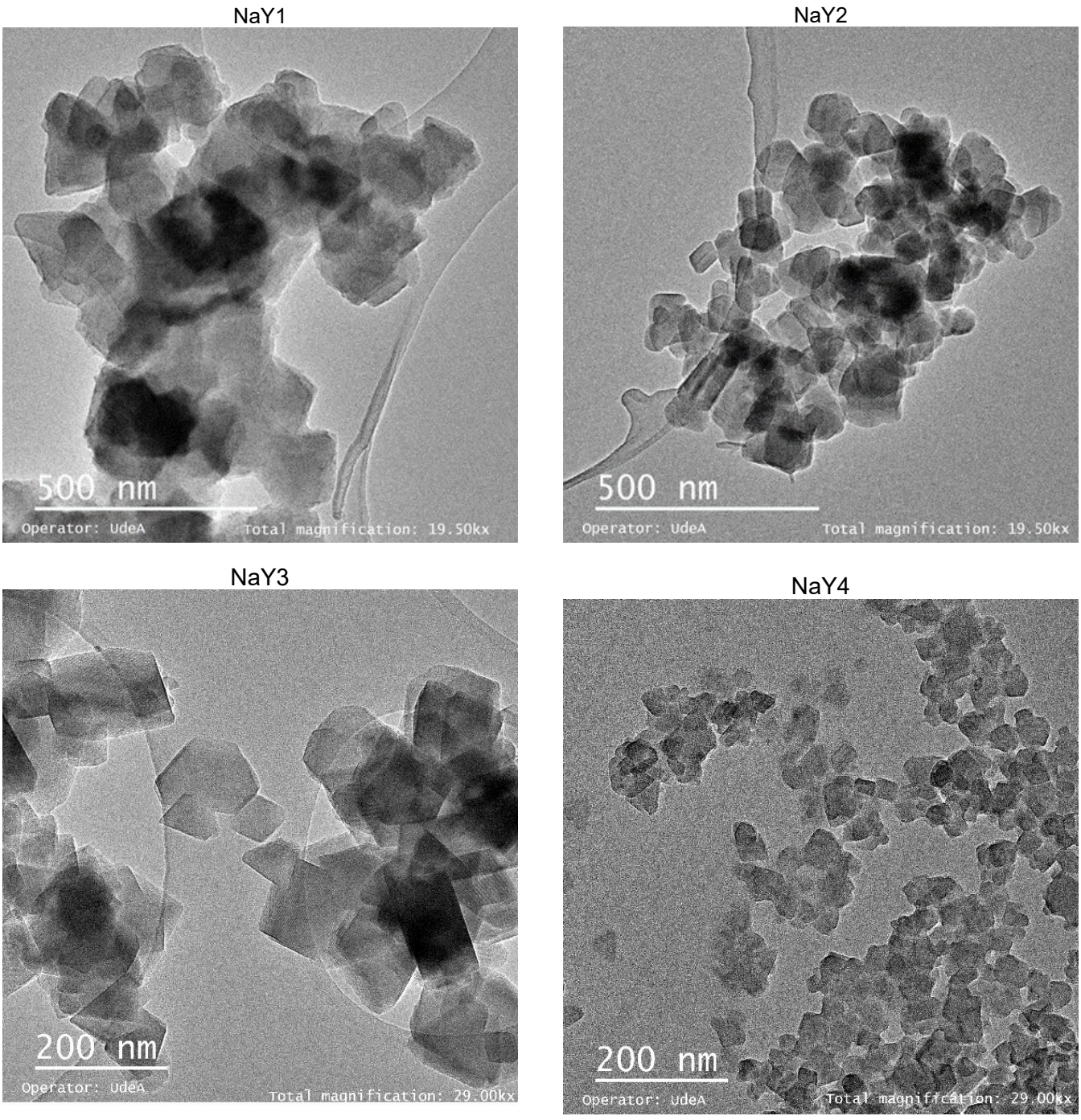

Figure S3. TEM images of synthesized zeolites NaY1, NY2, NaY3 and NaY4

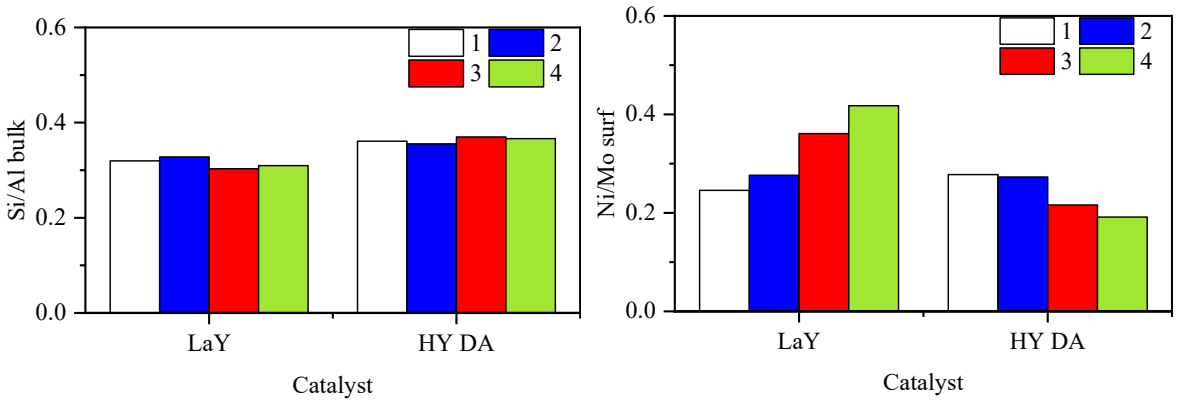

Figure S4. a) Bulk Si/Al and b) Ni/Mo ratio of the catalysts based on zeolites LaY and HY DA.

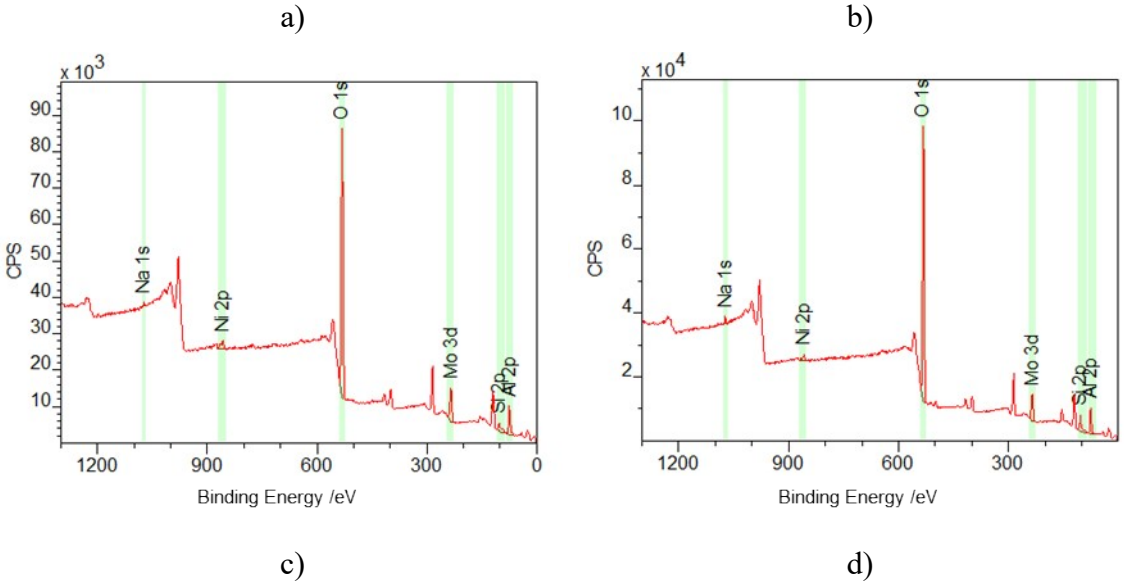

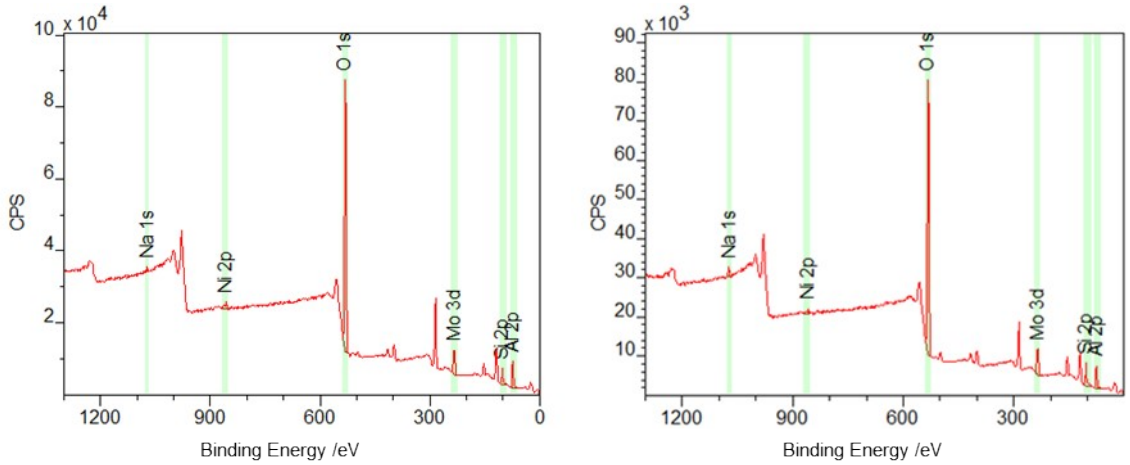

Figure S5. XPS spectra of a) HY1 DA, b) HY2 DA, c) HY3 DA, and d) HY4 DA catalysts.

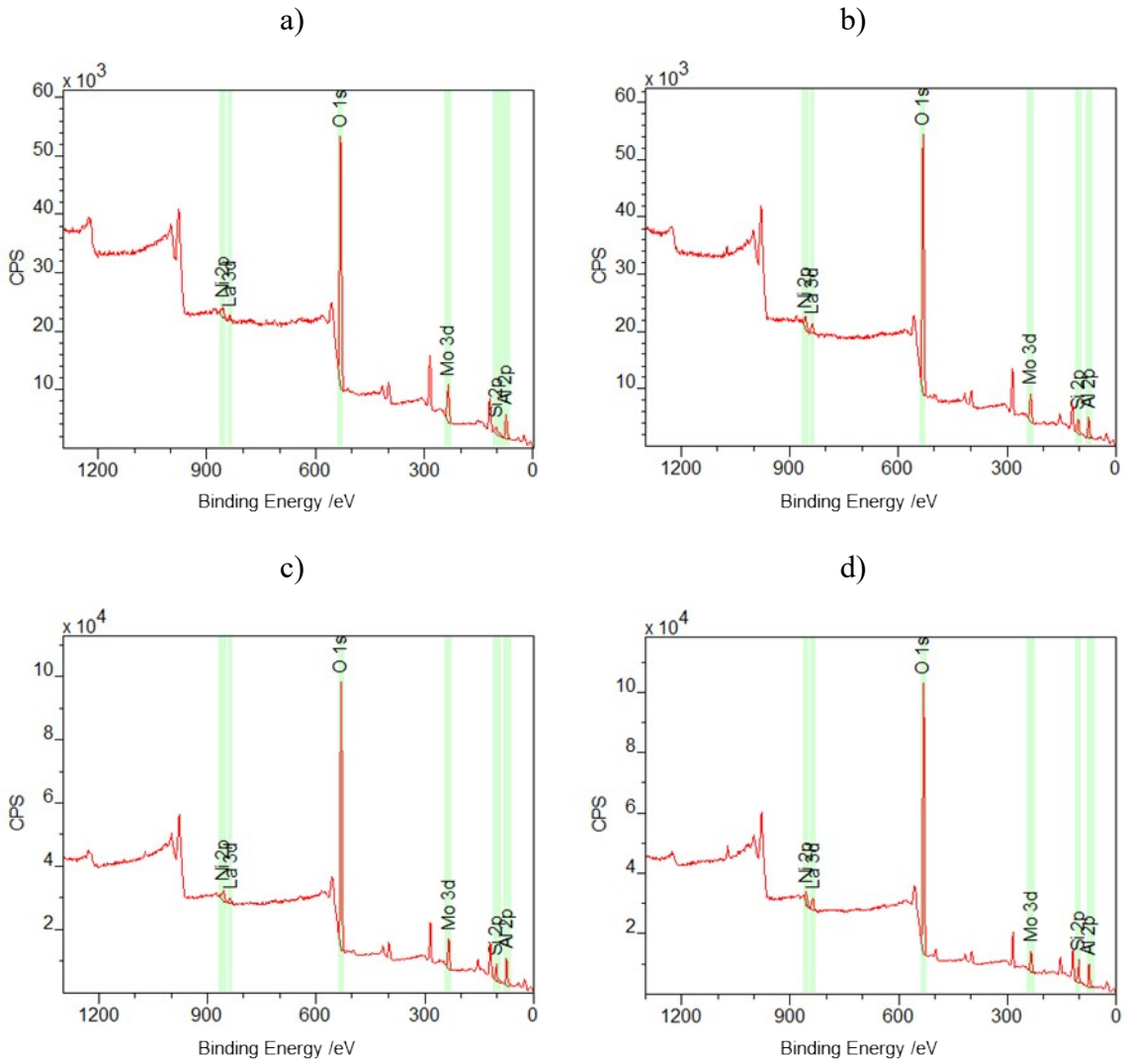

Figure S6. XPS spectra of a) LaY1, b) LaY2, c) LaY3, and d) LaY4 catalysts.

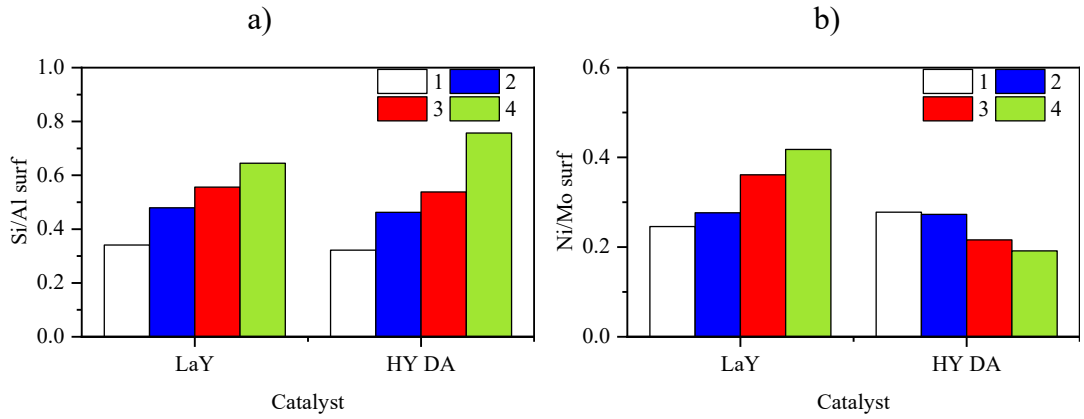

Figure S7. Surface Si/Al and Ni/Mo ratio of catalysts based on zeolites a) LaY and b) HY DA.

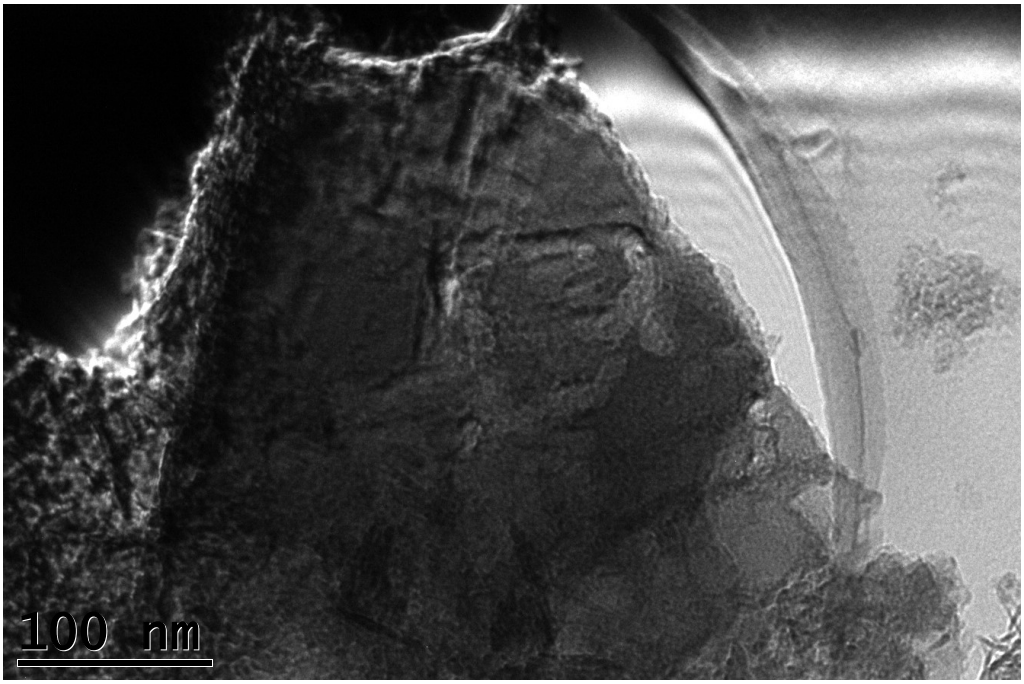

Figure S8. Dark-field TEM micrograph with oblique illumination of Cat. HY1 DA.

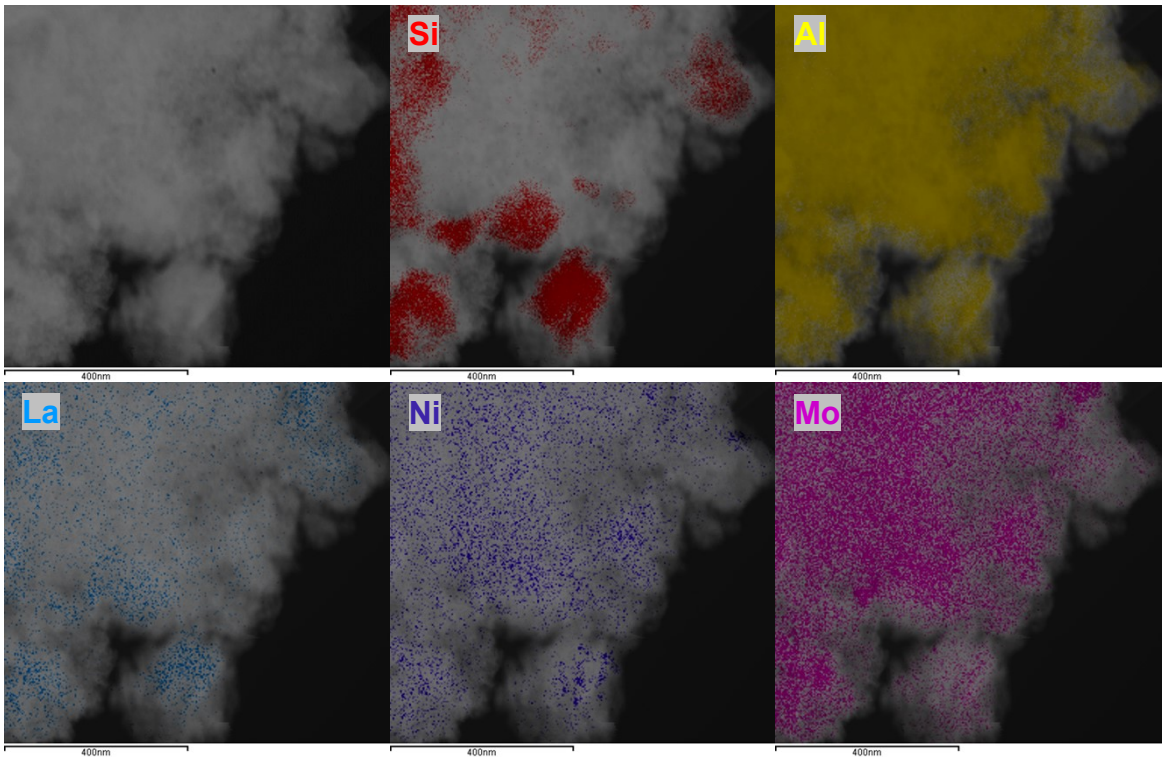

Figure S9. Element mapping catalyst NiMo/(LaY1 + Al_2O_3)

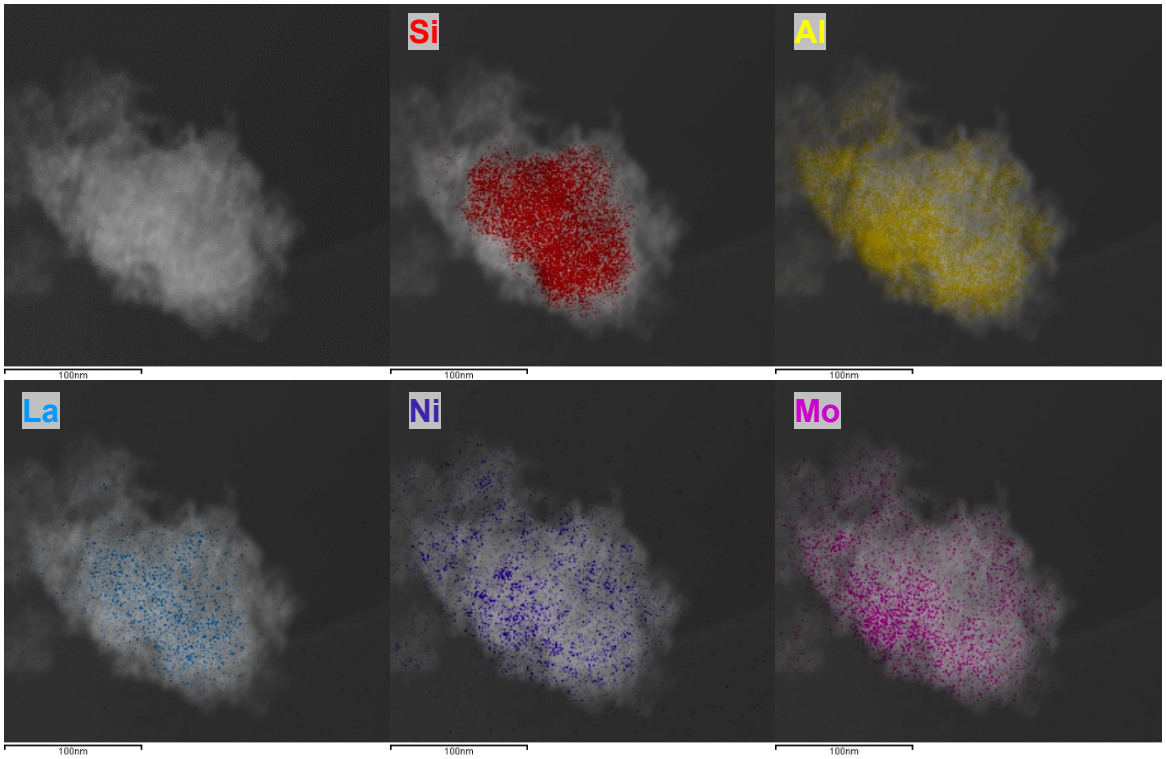

Figure S10. Element mapping catalyst NiMo/(LaY2 + Al_2O_3)

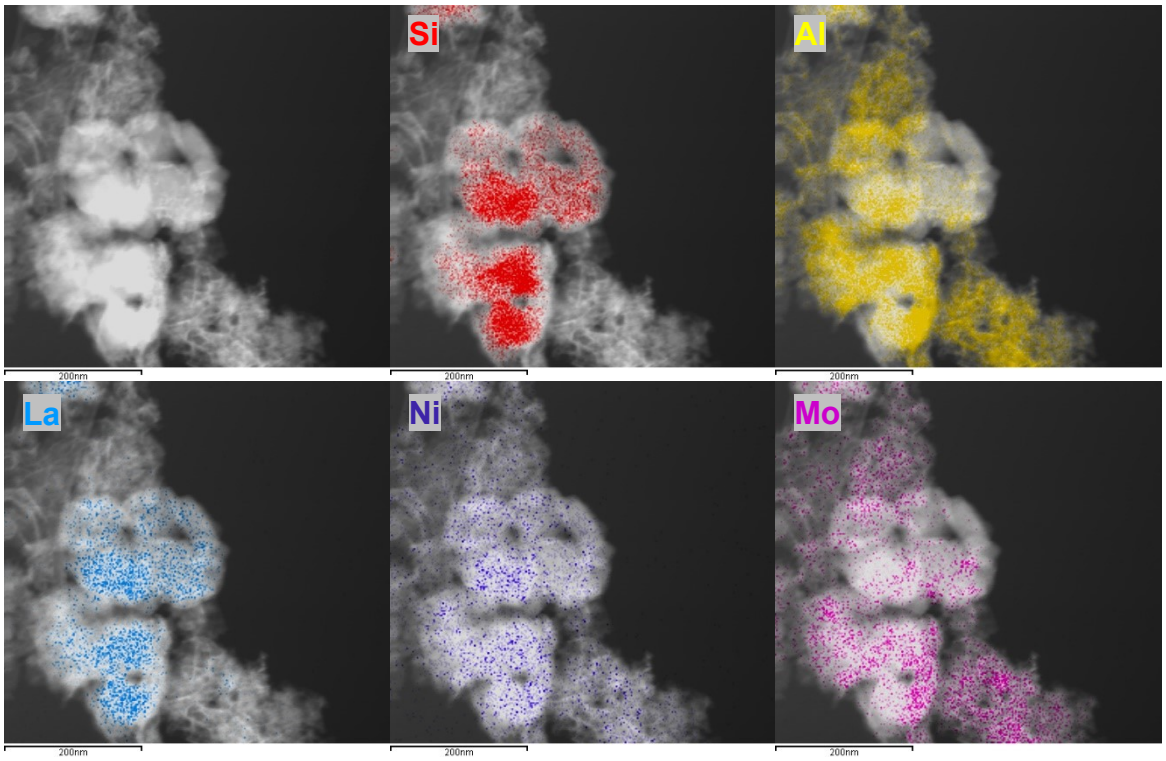

Figure S11. Element mapping catalyst NiMo/(LaY3 + Al_2O_3)

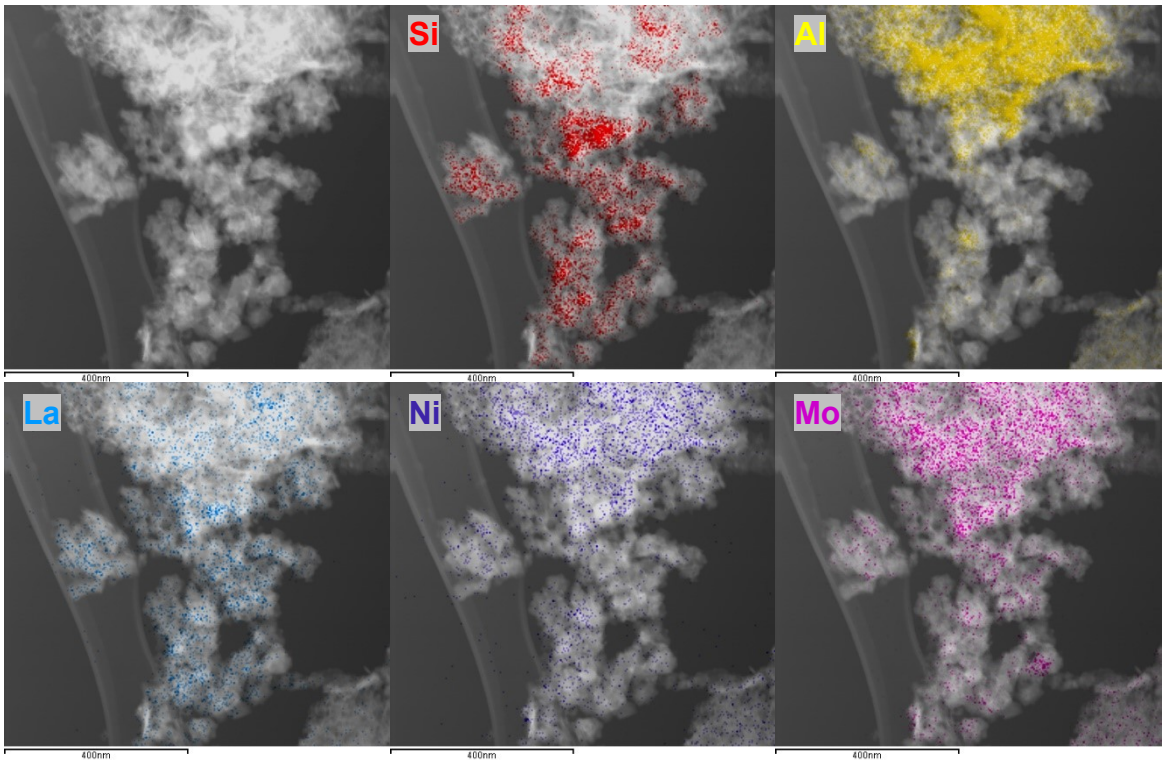

Figure S12. Element mapping catalyst NiMo/(LaY4 + Al_2O_3)

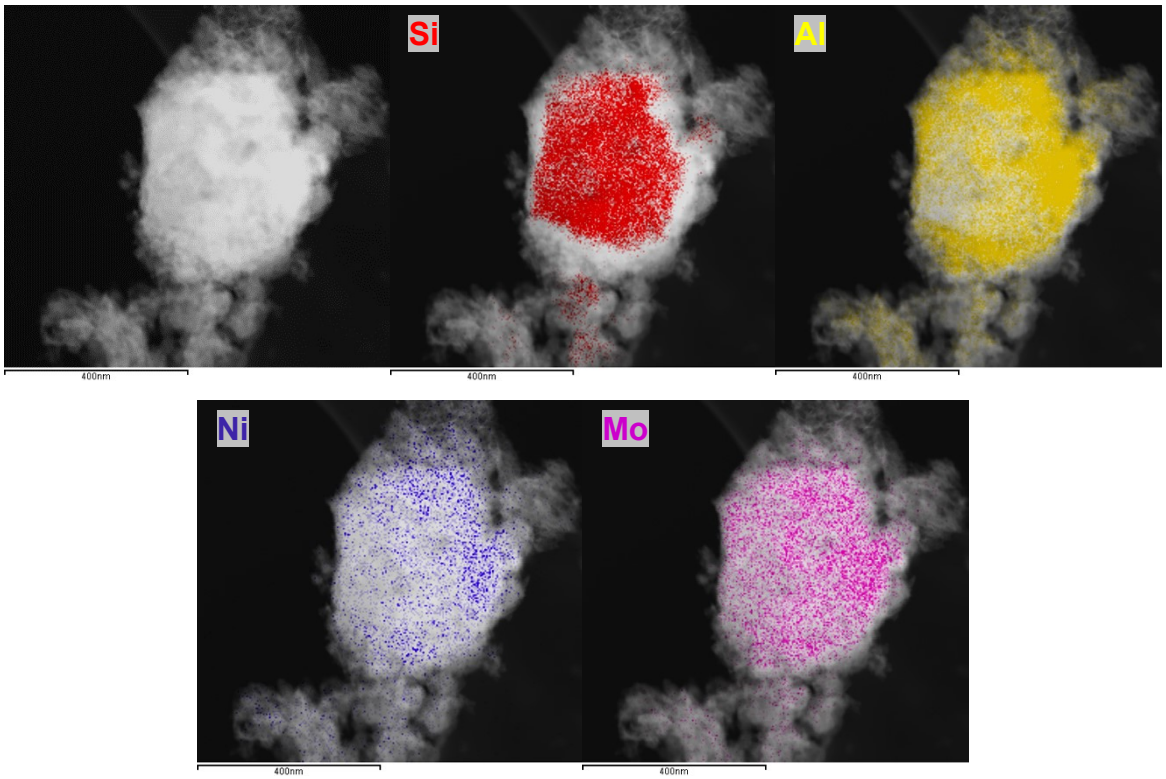

Figure S13. Element mapping catalyst NiMo/(HY1 DA+ Al_2O_3)

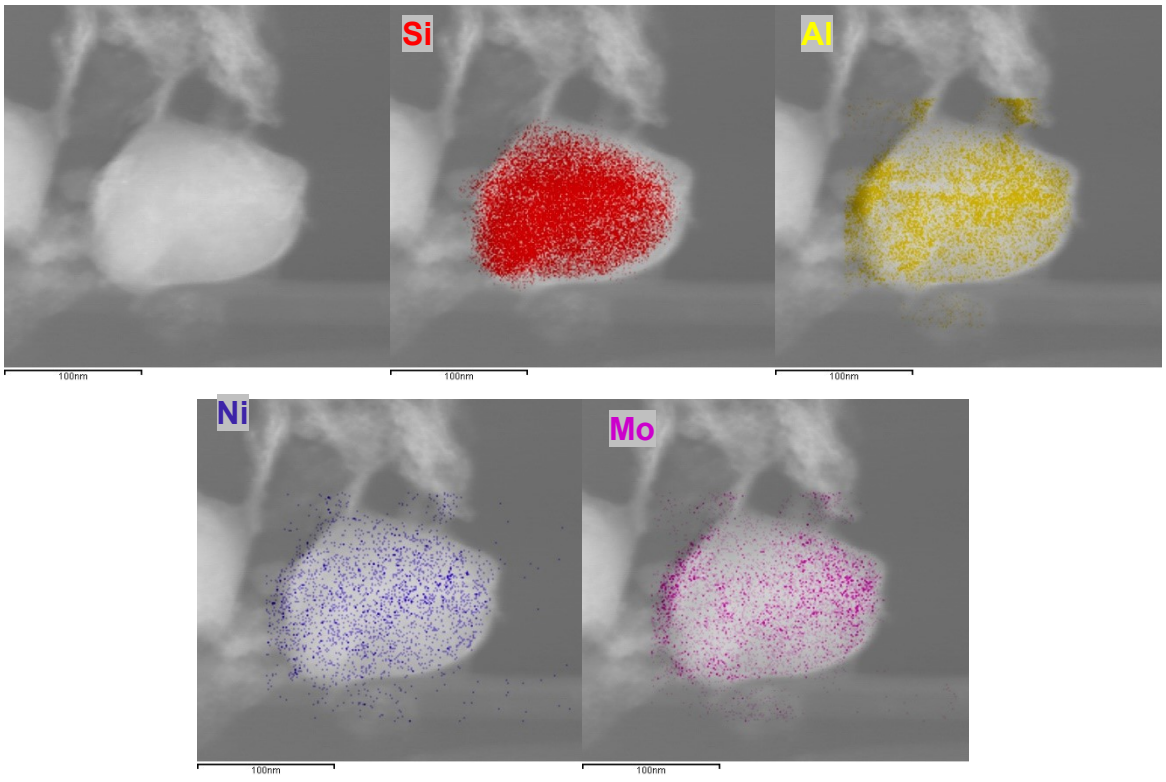

Figure S14. Element mapping catalyst NiMo/(HY2 DA+ Al_2O_3)

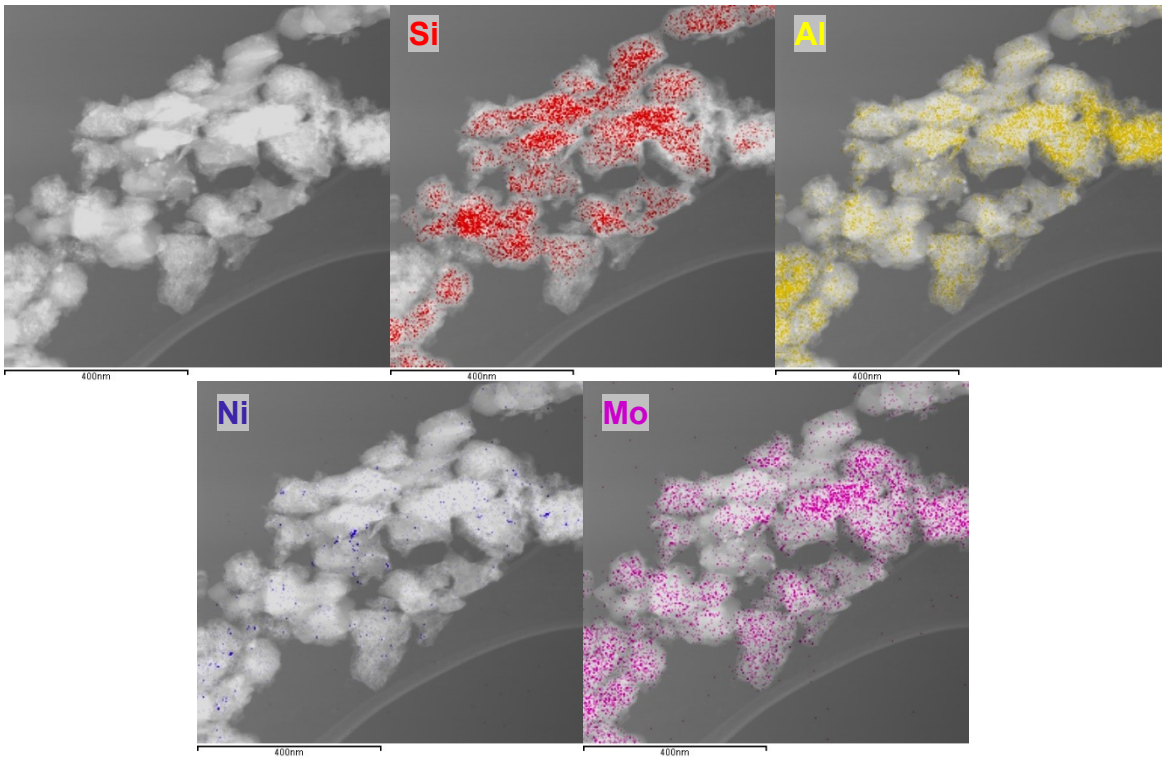

Figure S15. Element mapping catalyst NiMo/(HY3 DA+ Al_2O_3)

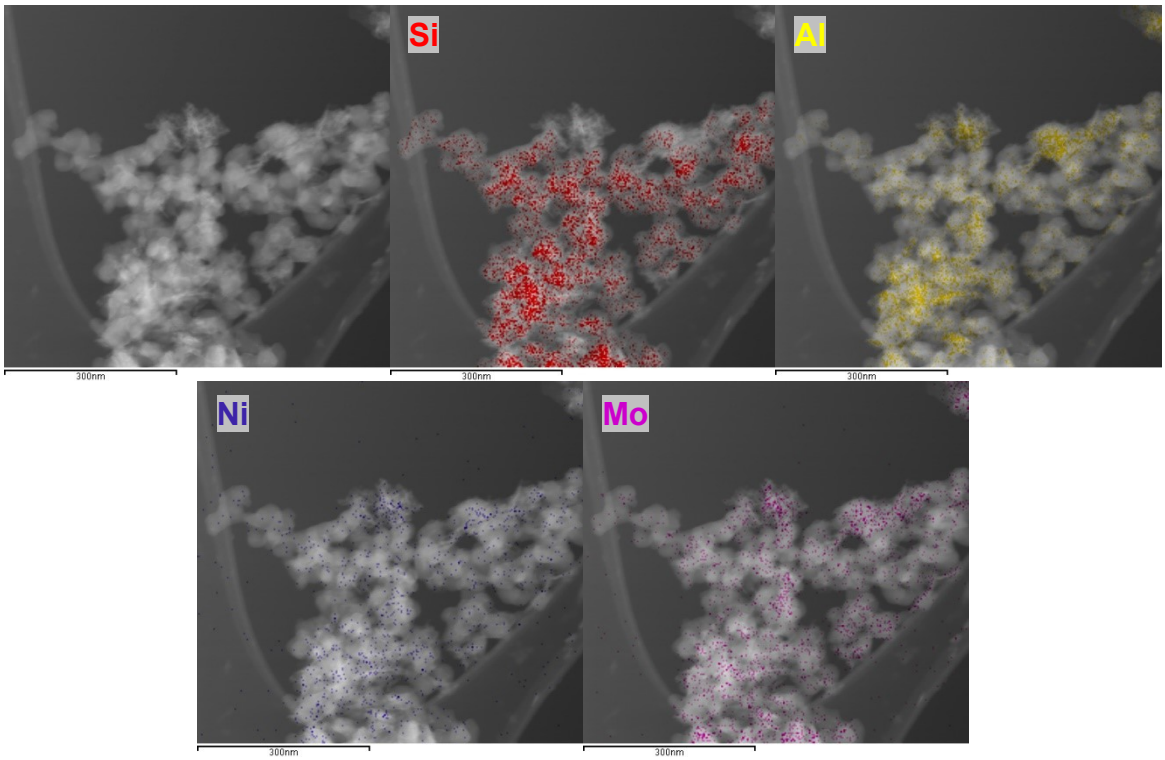

Figure S16. Element mapping catalyst NiMo/(HY4 DA+ Al_2O_3)

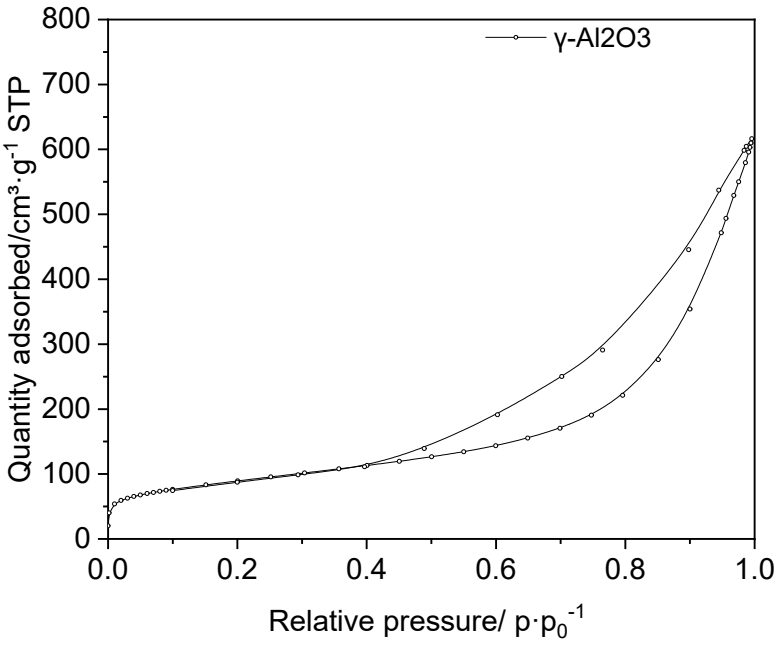

Figure S17. N2 isotherm of γ-Al_2O_3.

a) b)

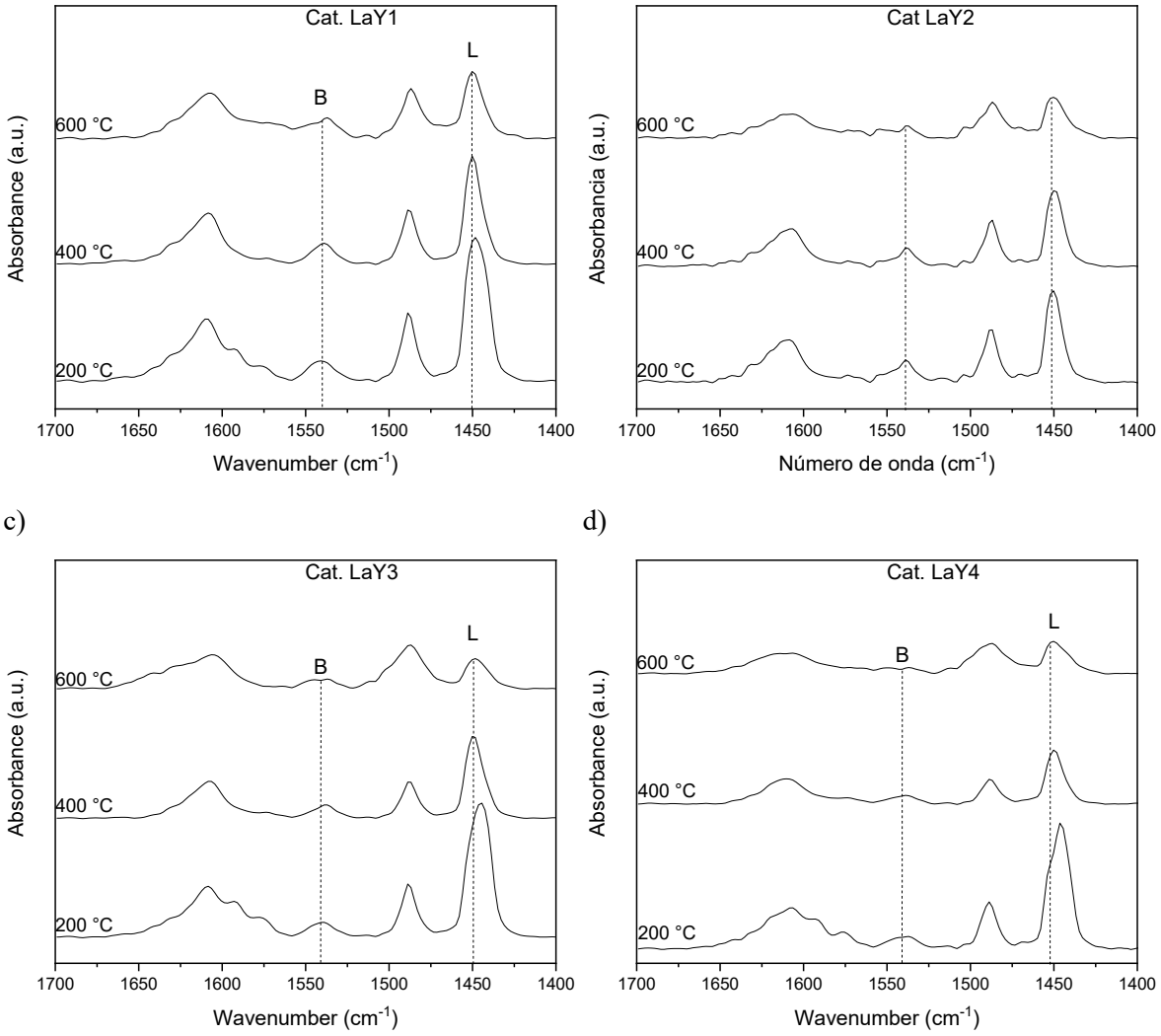

a) b) c) d)

Figure S18. IR-Py spectra of a) Cat. LaY1, b) Cat. LaY2, c) Cat. LaY3 and d) Cat. LaY4 from 200 °C to 400 °C

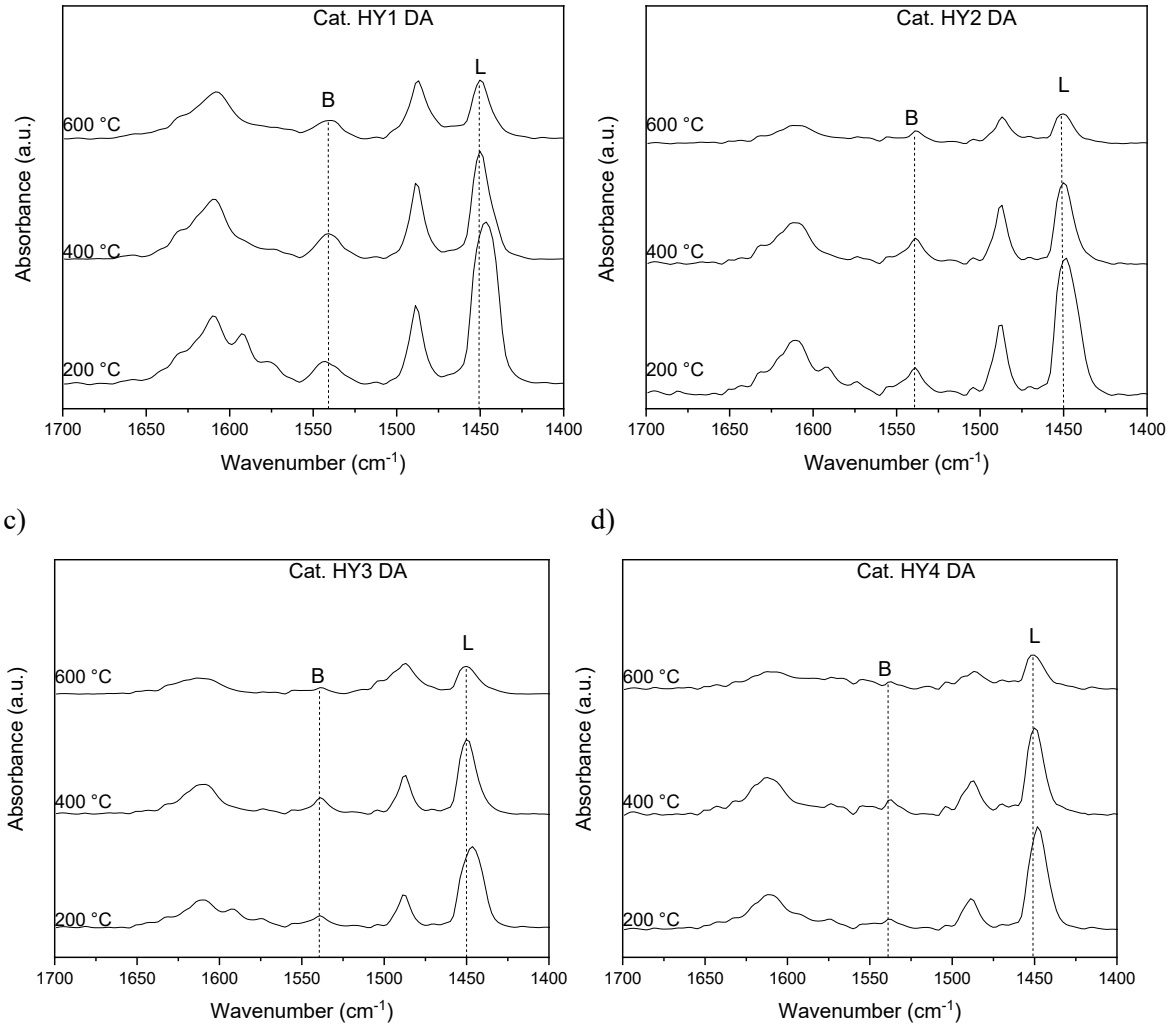

Figure S19. IR-Py spectra of a) Cat. HY1 DA, b) Cat. HY2 DA, c) Cat. HY3 DA and d) Cat. HY4 DA from 200 °C to 400 °C.

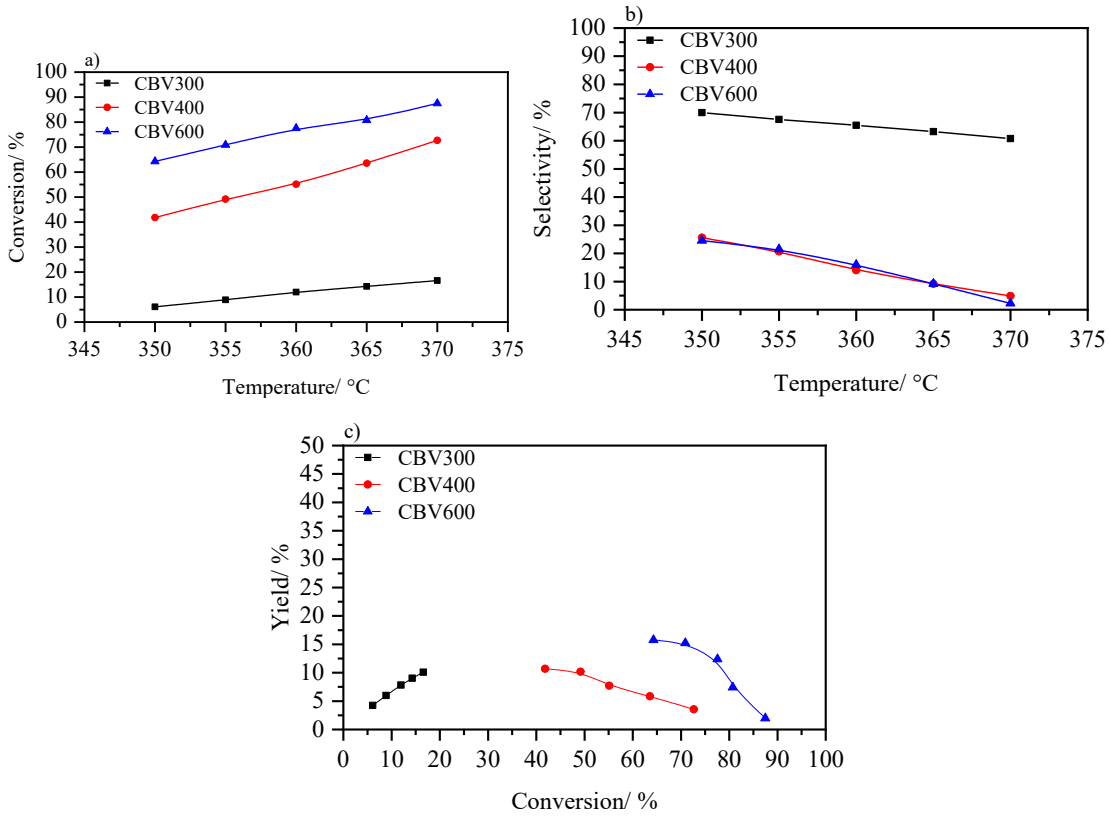

Figure S20. a) Conversion vs temperature, b) selectivity to middle distillates vs temperature y c) yield to distillates vs conversion to commercial catalysts CBV300, CBV400, CBV600.

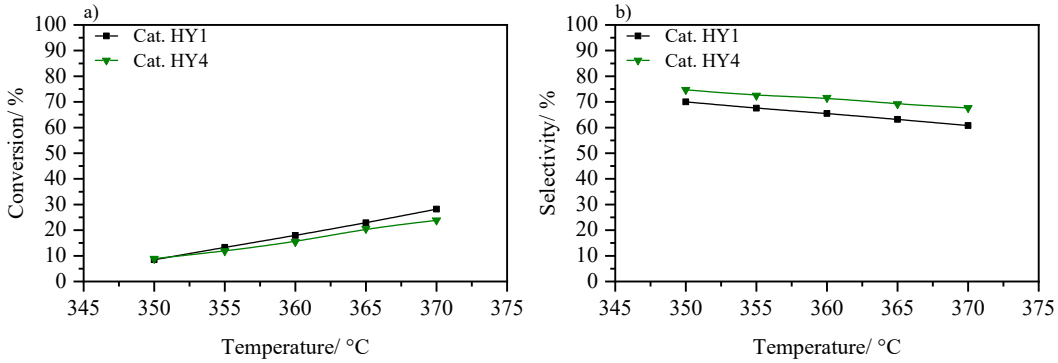

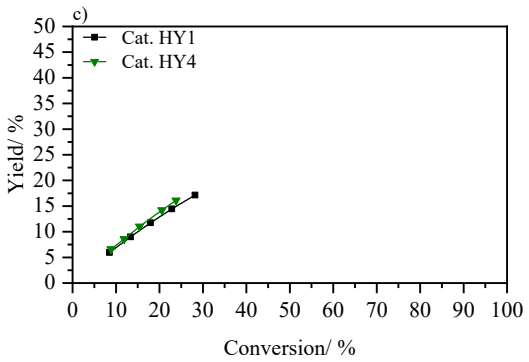

Figure S21. a) Conversion vs temperature, b) selectivity to middle distillates vs temperature y c) yield to distillates vs conversion to catalysts HY1 and HY4

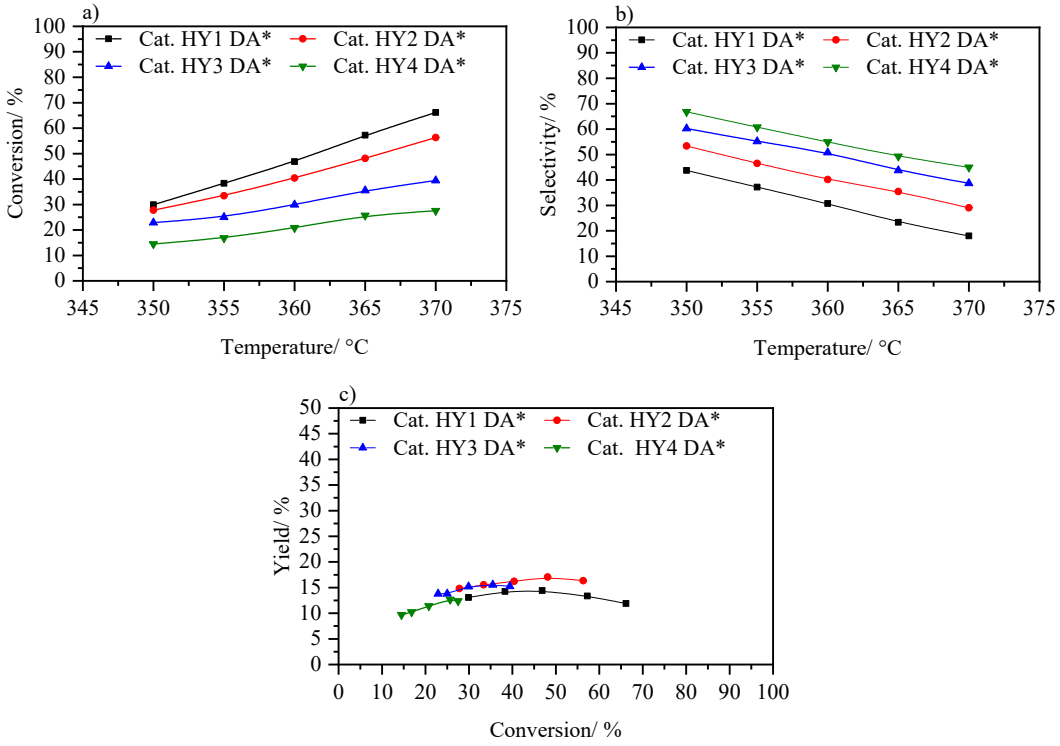

Figure S22. a) Conversion vs temperature, b) selectivity to middle distillates vs temperature y c) yield to distillates vs conversion to catalysts HY1 DA*, HY2 DA*, HY3 DA*, and HY4 DA*.

Table S1. Properties of Colombian vacuum gas oil

Properties	Value
Density /mg·ml^{-1}	0.91
S /ppm	43.0
N /ppm	25.0
Boiling range /°C	
IBP	277.5
5 %	357.6
10 %	374.0
20 %	393.6
30 %	409.9
40 %	424.2
50 %	437.6
60 %	451.5
70 %	466.8
80 %	482.9
90 %	502.9
95 %	518.0
FBP	548.0

Table S2: Temperature needed to reach maximum yield (wt.%) of middle distillates and corresponding selectivities in different cuts.

Catalysts	Temperature (°C)	Hydrocracking conversion (%wt)[a]	Selectivity (%wt)		Yield (%wt)	
			Naphtha[b]	Middle distillate[c]	Naphtha[b]	Middle distillate[c]
Cat. LaY1	360	46	27	40	12	18
Cat. LaY2	360	49	28	44	14	21
Cat. LaY3	360	41	26	46	10	19
Cat. LaY4	370	52	24	55	12	29
Cat. HY1 DA	360	41	26	46	10	19
Cat. HY2 DA	360	40	24	40	10	16
Cat. HY3 DA	365	36	20	44	7	16
Cat. HY4 DA	365	26	13	49	3	13

[a] Conversion % wt at the temperature where the maximum yield of middle distillates is achieved.

[b] Middle distillates: B.P in the range of 180–370 °C.

[c] Naphtha: B.P in the range of IPB–180 °C.